

A UNIVERSAL DECLINE LAW OF CLASSICAL NOVAE. II. GK PERSEI 1901 AND NOVAE IN 2005

IZUMI HACHISU

Department of Earth Science and Astronomy, College of Arts and Sciences, University of Tokyo, Komaba, Meguro-ku, Tokyo 153-8902, Japan

AND

MARIKO KATO

Department of Astronomy, Keio University, Hiyoshi, Kouhoku-ku, Yokohama 223-8521, Japan

to appear in the Astrophysical Journal, Supplement Series

ABSTRACT

Optical and infrared light-curves of classical novae are approximately homologous among various white dwarf (WD) masses and chemical compositions when free-free emission from optically thin ejecta is spherical and dominates the continuum flux of novae. Such a homologous template light-curve is called “a universal decline law.” Various nova light-curves are approximately reproduced from this universal law by introducing a timescaling factor which stretches or squeezes the template light-curve to match the observation. The timescale of the light curve depends strongly on the WD mass but weakly on the chemical composition, so we are able to roughly estimate the WD mass from the light-curve fitting. We have applied the universal decline law to the old nova GK Persei 1901 and recent novae that outburst in 2005. The estimated WD mass is $1.15 M_{\odot}$ for GK Per, which is consistent with a central value of the WD mass determined from the orbital velocity variations. The other WD masses of 10 novae in 2005 are also estimated to be $1.05 M_{\odot}$ (V2361 Cyg), $1.15 M_{\odot}$ (V382 Nor), $1.2 M_{\odot}$ (V5115 Sgr), $0.7 M_{\odot}$ (V378 Ser), $0.9 M_{\odot}$ (V5116 Sgr), $1.25 M_{\odot}$ (V1188 Sco), $0.7 M_{\odot}$ (V1047 Cen), $0.95 M_{\odot}$ (V476 Sct), $0.95 M_{\odot}$ (V1663 Aql), and $1.30 M_{\odot}$ (V477 Sct), within a rough accuracy of $\pm 0.1 M_{\odot}$. Four (V382 Nor, V5115 Sgr, V1188 Sco, and V477 Sct) of ten novae in the year 2005 are probably neon novae on an O-Ne-Mg WD. Each WD mass depends weakly on the chemical composition (especially the hydrogen content X in mass weight), i.e., the obtained WD masses increase by $+0.5(X-0.35) M_{\odot}$ for the six CO novae and by $+0.5(X-0.55) M_{\odot}$ for the four neon novae above. Various nova parameters are discussed in relation to its WD mass.

Subject headings: novae, cataclysmic variables — stars: individual (GK Persei) — stars: winds, outflows — white dwarfs

1. INTRODUCTION

Spectra of some novae are well fitted with that of free-free emission from optical to near infrared regions (e.g., Gallagher & Ney 1976; Kawara et al. 1976; Ennis et al. 1977, for V1500 Cyg). Hachisu & Kato (2006b, hereafter Paper I) developed a light curve model of novae in which free-free emission from optically thin ejecta dominates the continuum flux. They derived “a universal decline law” which is applicable to optical and near-infrared light-curves of various novae. Introducing “a timescaling factor” to their template nova light-curve, they showed that nova light curves are approximately reproduced only by a one-parameter family of the timescaling factor. Determining this timescaling factor, we are able to roughly predict various nova characteristic properties such as the hydrogen shell-burning phase, optically thick wind phase, ultraviolet burst phase, white dwarf (WD) mass, and duration of a supersoft X-ray phase (see Fig. 10 of Paper I), etc.

In Paper I, Hachisu & Kato applied this model to three well-observed classical novae, V1500 Cyg (Nova Cygni 1975), V1668 Cyg (Nova Cygni 1978), and V1974 Cyg (Nova Cygni 1992), and examined in detail the fitting in multiwavelength light-curves. They showed that these nova light curves are well fitted with the corresponding model light curves. As a result, they determined the WD mass in each object.

Here we further apply Hachisu & Kato’s “universal de-

cline law” to other classical novae. GK Per (Nova Persei 1901) is the first target in this paper, because it is an old nova the WD mass of which is reasonably well determined (Morales-Rueda et al. 2002). We also examine 10 new novae that are the all novae of which outburst is reported in 2005. In §2, we describe our method for model light curves. Our light curve analysis is presented for the old nova GK Per in §3, and for 10 new novae that outburst in 2005 in §4–13. Discussion and conclusions follow in §14 and §15, respectively.

2. THE MODEL OF FREE-FREE LIGHT CURVES

Classical novae are a result of a thermonuclear runaway on a mass-accreting white dwarf (WD) in a close binary system (e.g., Warner 1995, for a review). After a thermonuclear runaway sets in on a mass-accreting WD, its photosphere expands greatly and an optically thick wind mass-loss begins. The decay phase of novae can be followed by a sequence of steady state solutions (e.g., Kato & Hachisu 1994). In our nova light curve model, we assume that free-free emission of the optically thin ejecta dominates the continuum flux as in many classical novae (e.g., Gallagher & Ney 1976, for V1500 Cyg). The free-free emission of optically thin ejecta is estimated by

$$F_{\lambda} \propto \int N_e N_i dV \propto \int_{R_{ph}}^{\infty} \frac{\dot{M}_{wind}^2}{v_{wind}^2 r^4} r^2 dr \propto \frac{\dot{M}_{wind}^2}{v_{ph}^2 R_{ph}}, \quad (1)$$

during the optically thick wind phase (see Paper I for more details), where F_{λ} is the flux at the wavelength λ , N_e and N_i are

the number densities of electrons and ions, respectively, R_{ph} is the photospheric radius, \dot{M}_{wind} is the wind massloss rate, v_{ph} is the photospheric velocity, and $N_e \propto \rho_{\text{wind}}$ and $N_i \propto \rho_{\text{wind}}$. Here, we assume $v_{\text{wind}} = v_{\text{ph}}$ and use the relation of continuity, i.e., $\rho_{\text{wind}} = \dot{M}_{\text{wind}} / 4\pi r^2 v_{\text{wind}}$, where ρ_{wind} and v_{wind} are the density and velocity of the wind, respectively. These \dot{M}_{wind} , R_{ph} , and v_{ph} are calculated from our optically thick wind solutions (Kato & Hachisu 1994; Hachisu & Kato 2001b). The decline rate of the light curve, i.e., the evolutionary speed depends very sensitively on the WD mass (e.g., Kato 1999; Hachisu & Kato 2006a,b; Hachisu et al. 2006).

After the optically thick winds stop, the envelope settles into a hydrostatic equilibrium where its mass is decreasing by nuclear burning. When the nuclear burning decays, the WD enters a cooling phase, in which the luminosity is supplied with heat flow from the ash of hydrogen burning. We have followed nova evolution, using the same method and numerical techniques as those in Kato & Hachisu (1994) and Hachisu & Kato (2001b). After the optically thick wind stops, the total mass of ejecta is constant in time. For such homologously expanding ejecta, we have the flux of

$$F_{\lambda} \propto \int N_e N_i dV \propto \rho^2 V \propto \frac{M_{\text{ej}}^2}{V^2} V \propto R^{-3} \propto t^{-3}, \quad (2)$$

(e.g., Woodward et al. 1997), where ρ is the density, M_{ej} is the ejecta mass (M_{ej} is constant in time after the wind stops), R is the radius of the ejecta ($V \propto R^3$), and t is the time after the outburst.

We cannot uniquely specify the proportional constants in equations (1) and (2) because radiative transfer is not calculated outside the photosphere. Instead, we choose the constant to fit the light curve as shown below.

A schematic template light-curves obtained by Hachisu & Kato (2006b) is plotted in Figure 1. This template light curve for the universal law has a slope of the flux, $F \propto t^{-1.75}$, in the middle part (from ~ 2 to ~ 6 mag below the optical maximum) but it declines more steeply, $F \propto t^{-3.5}$, in the later part (from ~ 6 to ~ 10 mag), where t is the time after the outburst. Hachisu & Kato (2006b) adopted the time at the break point from the power of -1.75 to -3.5 , t_{break} , as “a time-scaling factor” of the light curve. After the optically thick wind stops, we have the flux of $F \propto t^{-3}$.

When a nova enters the transition/nebular phase, strong emission lines such as [O III] appear. The V magnitude becomes much brighter than that for the continuum flux due to the contribution of strong emission lines. In such a case, we lift up the template light-curve to approximate this effect as seen in Figure 1. The Strömgren medium bandpass y filter is designed to cut such strong emission lines and, as a result, the y magnitude follows well the light curve in Figure 1 (thick solid line) (see Figs. 12 and 18 of Hachisu & Kato 2006b, for such examples of V1500 Cyg and V1668 Cyg, respectively).

Table 1 shows 9 sets of chemical compositions assumed in our model. Although we had already calculated light curves of free-free emission for many sets of chemical compositions of nova envelopes in Paper I (see Table 2 of Paper I), we here add another set of chemical composition of $X = 0.65$, $X_{\text{CNO}} = 0.06$, and $Z = 0.02$ (CO nova 5 in Table 1) for GK Per, where X is the hydrogen content, X_{CNO} is the carbon, nitrogen, and oxygen content, X_{Ne} is the neon content, and Z is the heavy element content, each of them by mass weight.

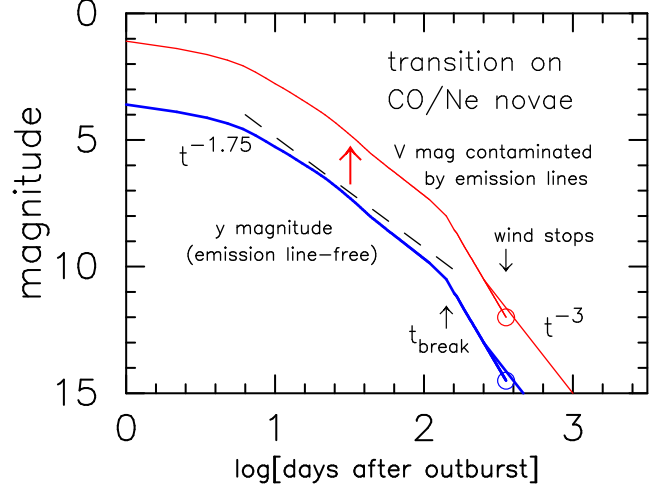


FIG. 1.— A schematic nova light curve with transition. Thick solid lines denote the light curves for continuum flux. The y magnitudes follow well these lines. Thin solid lines show the case in which strong emission lines begin to contribute to the nova light curve. The light curve gradually deviates. This occurs when the nova enters a transition phase (ignoring transition oscillations or a dust blackout) or a nebular phase. The popular wide-band V filters give a rather bright magnitude that may follow the thin lines in the later phase.

TABLE 1
CHEMICAL COMPOSITION OF THE PRESENT MODELS

novae case	X	X_{CNO}	X_{Ne}	Z^a	mixing ^b	comments
CO nova 1	0.35	0.50	0.0	0.02	100%	DQ Her
CO nova 2	0.35	0.30	0.0	0.02	...	GQ Mus
CO nova 3	0.45	0.35	0.0	0.02	55%	V1668 Cyg
CO nova 4	0.55	0.20	0.0	0.02	25%	PW Vul
CO nova 5	0.65	0.06	0.0	0.02	8%	QV Vul
Ne nova 1	0.35	0.20	0.10	0.02	...	V351 Pup
Ne nova 2	0.55	0.10	0.03	0.02	...	V1500 Cyg
Ne nova 3	0.65	0.03	0.03	0.02	...	QU Vul
Solar	0.70	0.0	0.0	0.02	0%	...

^a carbon, nitrogen, oxygen, and neon are also included in $Z = 0.02$ with the same ratio as solar abundance

^b mixing between the core material and the accreted matter with solar abundances

3. GK PER (NOVA PERSEI 1901)

We examine optical light curves of the 1901 outburst of GK Persei as an example of old fast novae, because its WD mass is reasonably well determined from the orbital velocity variations (Morales-Rueda et al. 2002) and it demonstrates an accuracy of our method. The 1901 outburst of GK Per was discovered by Anderson on February 21, 14.7 UT (JD 2415437.115) at the visual magnitude of 2.7 (e.g., Williams 1901a). The nova reached its visual maximum of 0.2 mag on February 22 UT. Williams (1901a) reported that the nova was not seen on the plate photographed on February 20, 11.5 UT (JD 2415435.979), 28 hours before the discovery, and should be fainter than twelfth magnitude. Therefore, we here regard February 20.5 UT (JD 2415436.0) as the outburst day.

3.1. Optical light curve

GK Per is a very old bright nova, so there are many literatures available, including a comprehensive summary of the visual light observations in Campbell (1903) and a comprehensive reference list in Sabbadin & Bianchini (1983). For the 1901 outburst, only visual and photographic magnitudes are available, which are plotted in Figure 2. The optical maximum was brief and the early decline was rather smooth. The

TABLE 2
 CHEMICAL ABUNDANCE OF GK PERSEI

object	H	CNO	Ne	Na-Fe	reference
Sun (solar)	0.71	0.014	0.0018	0.0034	Grevesse & Anders (1989)
GK Per 1901	0.54	0.036	0.0076	0.0024	Pottasch (1959)

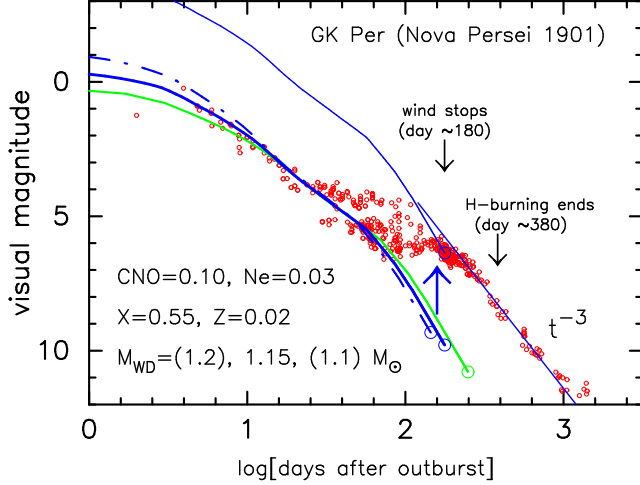


FIG. 2.— The best fit $1.15 M_{\odot}$ WD model (thick solid line) of free-free emission light curves is plotted together with $1.1 M_{\odot}$ (thin solid line) and $1.2 M_{\odot}$ (dash-dotted line) WD models. A straight line of $F_{\lambda} \propto t^{-3}$ is also added after the optically thick wind stops. Here we assume a chemical composition of $X = 0.55$, $X_{\text{CNO}} = 0.10$, $X_{\text{Ne}} = 0.03$, and $Z = 0.02$ (Ne nova 2 in Table 1). *Small open circles*: Visual and V observations taken from Child (1901), Gore (1901), Rambaut (1901a,b,c,d,e, 1902, 1903), Sharp (1901), and Williams (1901a,b,c,d, 1902, 1919). *Large open circles* at the lower ends of free-free light curves indicate the end points of optically thick winds. Two epochs of our best fit model are indicated by arrows: one is the epoch when the optically thick wind stops. The other is the epoch when the hydrogen shell-burning ends. When the nova enters a transition phase with oscillations, strong emission lines begin to contribute to nova visual light curves. So, the light curve gradually deviates from the template nova light curve. The transition phase ends when the optically thick wind stops. Then, the nova enters the nebular phase and the optical flux follows the free expansion law of $F_{\lambda} \propto t^{-3}$.

decline parameters are estimated to be $t_2 = 7$ and $t_3 = 13$ days (e.g. Downes & Duerbeck 2000), where t_2 and t_3 are the days during which the nova decays by 2 and 3 magnitudes from the optical maximum, respectively. There were prominent oscillations during the transition phase (from about day 25 to day 150 after the outburst) with a rough period of 3 days at first but later changing to 5 days with an amplitude of about one magnitude. The nova entered the nebular phase, after the transition phase ended at about day 170.

3.2. Chemical composition of ejecta

The chemical composition of the nova ejecta was estimated by Pottasch (1959) to be $X = 0.54$, $Y = 0.39$, $X_{\text{O}} = 0.036$, $X_{\text{Ne}} = 0.0076$, $X_{\text{S}} = 0.0022$, and $X_{\text{Ca}} = 0.00022$. Here Y is the helium content, X_{O} is the oxygen content, X_{S} is the sulfur content, and X_{Ca} is the calcium content, each of them by mass weight.

Such mild enhancement of neon by a factor of $\sim 3-4$ (see Table 2) can occur through production of ^{22}Ne during the helium-burning phase in the precursor red giant of the WD (e.g., Livio & Truran 1994). The CNO cycle converts most of the initial carbon, nitrogen, and oxygen isotopes into ^{14}N . During the ensuing helium-burning phase, this ^{14}N is transformed into ^{22}Ne by $^{14}\text{N}(\alpha, \gamma)^{18}\text{F}(e^+ \nu)^{18}\text{O}(\alpha, \gamma)^{22}\text{Ne}$. If

outward mixing of core material is the source of the heavy element-enrichment observed in nova ejecta, then a ^{22}Ne enrichment accompanies any CNO enrichment. Therefore, neon and CNO enrichment of a factor $\sim 3-4$, as tabulated in Table 2, does not directly mean that the underlying WD is a O-Ne-Mg white dwarf. We suppose, in the present paper, that the underlying WD in GK Per is not an ONeMg white dwarf but a carbon-oxygen (CO) white dwarf.

3.3. Light curve fitting in the decay phase

It has been extensively discussed, in Paper I, that nova light curves based on free-free emission depend sensitively on the WD mass and also weakly on the chemical composition of the envelope, i.e., on the X and X_{CNO} (but hardly on the X_{Ne}), because these two are main players in the CNO cycle (but neon is not). First assuming a chemical composition of $X = 0.55$, $X_{\text{CNO}} = 0.10$, $X_{\text{Ne}} = 0.03$, and $Z = 0.02$ for a typical neon nova (case Ne nova 2 in Table 1), we obtain a best fit light curve as plotted in Figure 2. The WD mass is estimated to be $1.15 M_{\odot}$ with a fitting accuracy of $\pm 0.05 M_{\odot}$. The visual magnitudes are nicely fitted with our model light curve after the optical maximum, at least, until about day 25. Strong emission lines of [O III] appeared, 4363 Å on JD 2415464.0 (day 24) and 5007 Å on JD 2415468.0 (day 28) (see, e.g., McLaughlin 1949; Payne-Gaposchkin 1957), when the oscillation began. The latter 5007 Å contributed to the visual magnitude, so it begins to deviate from our model light curve after the fluctuation began, as seen in Figure 2.

Usually the V magnitudes become much brighter than that for the continuum flux due to the contribution of strong emission lines such as [O III] mentioned above. In such a case, we lift up the template light-curve to approximate this effect as seen in Figures 1 and 2. If we use the Strömgren medium bandpass y filter, which is designed to cut such strong emission lines, the y magnitudes probably follow well the light curve in Figure 1 (thick solid line). This effect is also discussed in Paper I for V1500 Cyg and V1668 Cyg.

Next we examine how the estimated WD mass depends on the assumed chemical composition of a nova envelope. Assuming a different chemical composition of $X = 0.65$, $X_{\text{CNO}} = 0.06$, and $Z = 0.02$ for a less heavy element-enhanced CO nova, we obtain a best-fit light curve for a WD mass of $1.2 M_{\odot}$. We have also added a case of $X = 0.35$, $X_{\text{CNO}} = 0.30$, and $Z = 0.02$ (case CO nova 2 in Table 1) for a much more heavy element-enhanced CO nova and obtained a best-fit one for a WD mass of $1.05 M_{\odot}$. From these results, we may estimate the WD mass to be

$$M_{\text{WD}}(X) \approx M_{\text{WD}}(0.55) + 0.5(X - 0.55), \quad (3)$$

when $0.35 \leq X \leq 0.65$ and $0.03 \leq X_{\text{CNO}} \leq 0.35$. Here $M_{\text{WD}}(0.55)$ means the WD mass estimated for $X = 0.55$. It should be noted that the decline rates of nova light-curves depend strongly on the WD mass and weakly on the X and X_{CNO} but hardly on the X_{Ne} .

To summarize, we may conclude that the WD mass is $M_{\text{WD}} = 1.15 \pm 0.05 M_{\odot}$ for $X = 0.54$ (Pottasch 1959).

3.4. Discussion on the results for GK Per

Morales-Rueda et al. (2002) obtained the mass ratio of the binary components by assuming that the absorption line width is due to the rotational broadening of the K subgiant companion, that is, $q \equiv M_{\text{K}}/M_{\text{WD}} = 0.55 \pm 0.21$, where M_{K} is the

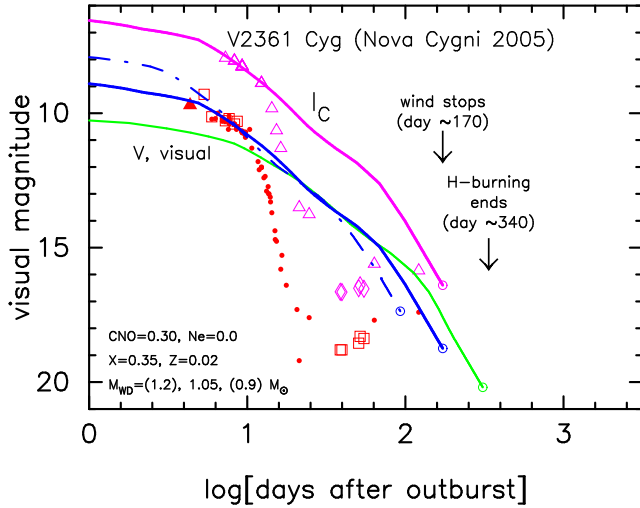


FIG. 3.— The best fit $1.05 M_{\odot}$ WD model (thick solid line) is plotted together with $0.9 M_{\odot}$ (thin solid line) and $1.2 M_{\odot}$ (dash-dotted line) WD models. Here we assume a chemical composition of $X = 0.35$, $X_{\text{CNO}} = 0.30$, and $Z = 0.02$ (CO nova 2 in Table 1). Dots: visual and V observations taken from AAVSO. Open squares: visual and V observations taken from IAU Circulars 8483, 8487, and 8511. Open triangles: I_C magnitude observations taken from AAVSO. Open diamonds: Sloan i' magnitude observations taken from IAU Circular 8511. The discovery magnitude on a film given by Nishimura (Nakano et al. 2005c) is indicated by a filled triangle.

mass of the K subgiant. Since the semi-amplitude of the radial velocity is $K_K = 120.5 \pm 0.7 \text{ km s}^{-1}$ for the K subgiant companion, we have a relation of

$$M_{\text{WD}} = \frac{0.36(1+q)^2}{\sin^3 i} M_{\odot}, \quad (4)$$

The inclination angle of the binary should be lower than $i < 73^\circ$ because no eclipses were observed in GK Per (Reinsch 1994). On the other hand, the orbital inclination was estimated, from a correlation between emission-line width and accretion disk inclination, to be $\sim 75^\circ$ (Warner 1986), close to the upper limit. If we fix the mass ratio of $q = 0.55$ at its central value, then we obtain $M_{\text{WD}} = 1.0 M_{\odot}$ for $i = 73^\circ$, $M_{\text{WD}} = 1.1 M_{\odot}$ for $i = 68^\circ$, and $M_{\text{WD}} = 1.2 M_{\odot}$ for $i = 63^\circ$. These estimated WD masses are very consistent with our fitting results and demonstrate an accuracy ($\pm 0.1 M_{\odot}$) of our method.

On the other hand, CO white dwarf masses born in a binary have been calculated by Umeda et al. (1999) to be $M_{\text{CO}} \lesssim 1.07 M_{\odot}$, for various metallicities. If the WD of GK Per is a $1.15 M_{\odot}$ CO core, this Umeda et al.'s result suggests that the WD had grown up by accretion from the evolved companion.

Slavin et al. (1995) derived a distance of 0.455 ± 0.03 kpc from an expansion parallax of the nova shell. Slavin et al. assumed an expansion velocity of 1200 km s^{-1} (Cohen & Rosenthal 1983) for a $103''$ wide nova shell (i.e., $d = 92.5 \times 365 \times 24 \times 60 \times 60 \times 1200 \times 10^5 / 1.5 \times 10^{13} / 51.5 = 453 \text{ pc}$). Wu et al. (1989) derived an $E(B-V) = 0.3 \pm 0.05$. Therefore, the absolute magnitude is $M_{V,\text{max}} = -9.0 \pm 0.3$ for the apparent maximum magnitude of $m_{V,\text{max}} = 0.2$. Since the Eddington luminosity of a $1.15 M_{\odot}$ WD is estimated to be $M_{V,\text{Edd}} = -6.0$ for OPAL opacity from our model, the maximum brightness of GK Per is super-Eddington by about 3 mag.

4. V2361 CYG (NOVA CYGNI 2005)

The outburst of V2361 Cygni was discovered by Nishimura on 2005 February 10.85 UT (JD 2453412.35) at mag ≈ 9.7

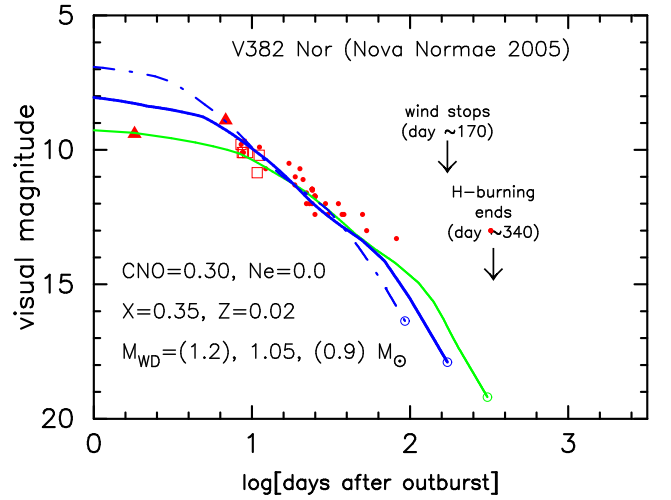


FIG. 4.— The best fit $1.05 M_{\odot}$ WD model (thick solid line) is plotted together with $0.9 M_{\odot}$ (thin solid line) and $1.2 M_{\odot}$ (dash-dotted line) WD models. Here we assume a chemical composition of $X = 0.35$, $X_{\text{CNO}} = 0.30$, and $Z = 0.02$ for a CO nova. Dots: Visual and V observations taken from AAVSO. Open squares: Visual and V observations taken from IAU Circulars 8497 and 8498. Filled triangles: red magnitudes given by Liller (Liller et al. 2005b).

(Nakano et al. 2005c). Because the star was not detected (limiting mag 11) on 2005 February 6, we assume that JD 2453408.0 (February 6.5 UT) is the outburst day. Adopting an visual magnitude of 9.3 on JD 2453413.3 observed by Wakuda (Nakano et al. 2005c) as the maximum visual magnitude for V2361 Cyg, we obtain $t_2 = 6$ days and $t_3 = 8$ days. The light curve is plotted in Figure 3, which is strongly affected by dust formation.

Since the $H\alpha/H\beta$ intensity ratio is consistent with the high reddening (Russell et al. 2005b) and the V and I_C magnitudes sharply decayed by dust blackout, we regard that this nova is a CO nova. Our best-fit light curves are plotted in Figure 3 for a CO nova chemical composition of $X = 0.35$, $X_{\text{CNO}} = 0.30$, and $Z = 0.02$. The deep blackout by dust formation started two weeks after the outburst, so that we can fit it with our model light curve only during the first 10 days of the visual (V) and I_C magnitudes. The WD mass is estimated to be $1.05 \pm 0.15 M_{\odot}$.

Venturini et al. (2005) reported that the near-infrared excess had diminished about 280 days after the outburst, indicating that a dust shell formed after outburst has dissipated. This suggests that an optically thick nova wind has already stopped long before this observational epoch, because dust formation continues during the optically thick wind phase. Our model ($M_{\text{WD}} = 1.05 M_{\odot}$) predicts that the optically thick wind stopped 170 days after the outburst, being consistent with the infrared observation.

5. V382 NOR (NOVA NORMAE 2005)

The outburst of V382 Normae was discovered by Liller on 2005 March 13.309 UT (JD 2453442.809) at mag ≈ 9.4 (Liller et al. 2005b), including no detection of this nova (limiting mag 11) on 2005 March 9 (JD 2453438.5). So we assume that March 11.5 UT (JD 2453441.0) is the outburst day. Adopting an visual magnitude of 8.9 on JD 2453447.8 (Liller et al. 2005b) as the maximum visual magnitude, we obtain $t_2 = 12$ days and $t_3 = 18$ days.

Our best-fit light curves are plotted in Figure 4 for a chemical composition of CO nova 2, $X = 0.35$, $X_{\text{CNO}} = 0.30$, and $Z = 0.02$. The visual (V) magnitudes are roughly fitted with

TABLE 3
 LIGHT CURVE PARAMETERS OF FOUR OLD NOVAE

object	WD mass (M_{\odot})	t_2 (days)	t_3 (days)	t_{break} (days)	t_{wind} (days)	$t_{\text{H-burning}}$ (days)	reference for t_2 and t_3
GK Per 1901	1.15 ± 0.05	7	13	73	182	382	Downes & Duerbeck (2000)
V1500 Cyg 1975	1.15	2.9	3.6	70	180	380	Warner (1995)
V1668 Cyg 1978	0.95	12.2	24.3	110 ^a	280	720	Mallama & Skillman (1979)
V1974 Cyg 1992	1.08 ^b	16	42	96	250	600	Warner (1995)

^a $t_{\text{break}} = 86$ days in Table 11 of Hachisu & Kato (2006b, Paper I) is not correct and it should be replaced with $t_{\text{break}} = 110$ days

^b $M_{\text{WD}} = 1.08 M_{\odot}$ is adopted here to reproduce the observational supersoft X-ray phase (Krautter et al. 1996)

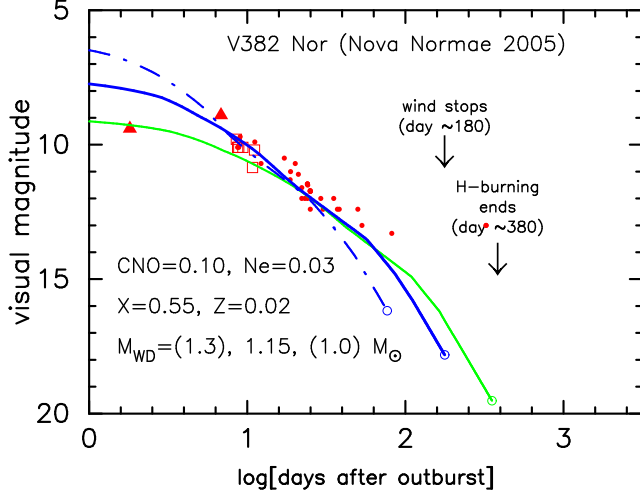


FIG. 5.— Same as in Fig. 4, but calculated light curves for a neon nova composition of $X = 0.55$, $X_{\text{CNO}} = 0.10$, $X_{\text{Ne}} = 0.03$, and $Z = 0.02$ (model Ne nova 2). The best fit $1.15 M_{\odot}$ WD model (thick solid line) is plotted together with $1.0 M_{\odot}$ (thin solid line) and $1.3 M_{\odot}$ (dash-dotted line) WD models.

our model light curve. It should be noted that Liller provided the red magnitudes (with an orange filter) for the first two points (filled triangles). The WD mass is estimated to be $1.05 \pm 0.15 M_{\odot}$. Since this estimated WD mass is very close to the upper limit for CO white dwarf masses born in a binary, i.e., $M_{\text{CO}} \lesssim 1.07 M_{\odot}$ (e.g., Umeda et al. 1999), so that we introduce an O-Ne-Mg core instead of a CO core. Another best fit model is obtained for a chemical composition of $X = 0.55$, $X_{\text{CNO}} = 0.10$, $X_{\text{Ne}} = 0.03$, and $Z = 0.02$. The visual (V) magnitudes are roughly fitted with the observation when the WD mass is $1.15 \pm 0.15 M_{\odot}$ as shown in Figure 5. We obtain a higher WD mass because we assume a higher hydrogen content and a lower enhancement of the CNO elements.

6. V5115 SGR (NOVA SAGITTARII 2005)

The outburst of V5115 Sagittarii was independently discovered by Nishimura and Sakurai on 2005 March 28.8 UT (JD 2453458.3) at mag ≈ 8.7 and 9.1 (Nakano et al. 2005b), respectively. Yamaoka noted that nothing is visible at this location on an ASAS-3 image taken on March 27.464 UT (JD 2453456.964) with limiting mag about 14 (Nakano et al. 2005b). Therefore we assume that JD 2453457.0 (March 27.5 UT) is the outburst day. Adopting an visual magnitude of 7.8 on JD 2453459.2 observed by Wakuda (Nakano et al. 2005a) as the maximum visual magnitude for V5115 Sgr, we obtain $t_2 = 7$ days and $t_3 = 14$ days.

Our light-curve fitting is shown in Figure 6 for CO nova 2, $X = 0.35$, $X_{\text{CNO}} = 0.30$, and $Z = 0.02$. The visual (V) magnitudes are nicely fitted with our model light curve until about day 40. This indicates that the contribution of emission lines to the V bandpass is not so large until about day 40. The

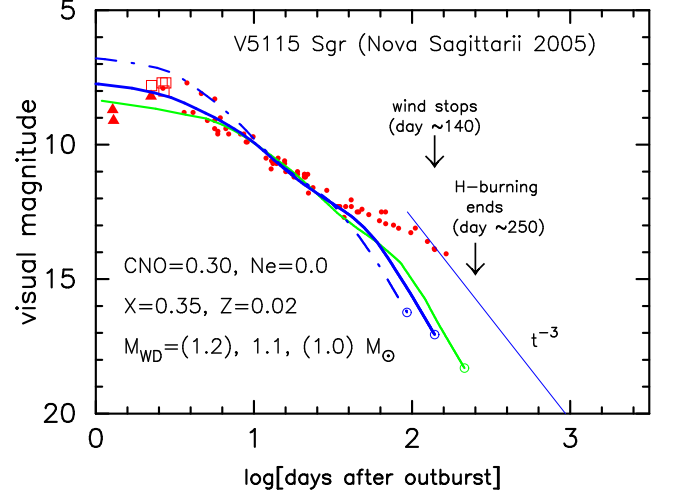


FIG. 6.— The best fit $1.1 M_{\odot}$ WD model (thick solid line) is plotted together with $1.0 M_{\odot}$ (thin solid line) and $1.2 M_{\odot}$ (dash-dotted line) WD models. A straight line of $F_{\lambda} \propto t^{-3}$ is also added after the optically thick wind stops. Here we assume a chemical composition of $X = 0.35$, $X_{\text{CNO}} = 0.30$, and $Z = 0.02$ for a CO nova (model CO nova 2). Dots: visual and V magnitudes taken from AAVSO. Open squares: visual and V observations taken from IAU Circulars 8500, 8501, and 8502. Filled triangles: discovery magnitudes on a film and a non-filtered CCD in a digital camera taken from IAU Circular 8500.

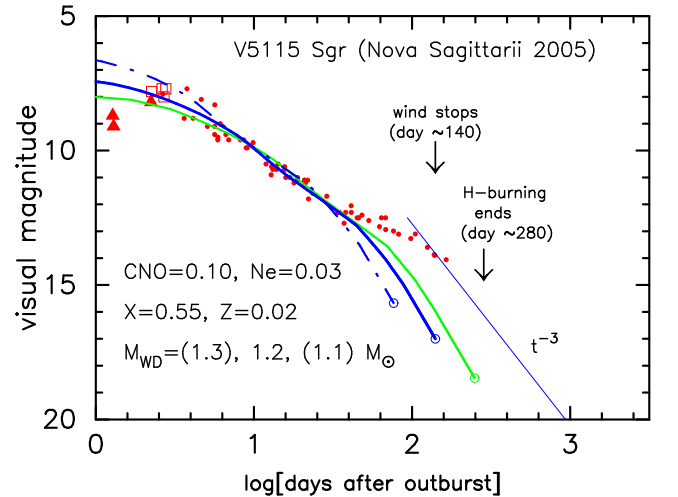


FIG. 7.— Same as in Fig. 6, but for neon novae with a chemical composition of $X = 0.55$, $X_{\text{CNO}} = 0.10$, $X_{\text{Ne}} = 0.03$, and $Z = 0.02$ (model Ne nova 2). The best fit $1.2 M_{\odot}$ WD model (thick solid line) is plotted together with $1.1 M_{\odot}$ (thin solid line) and $1.3 M_{\odot}$ (dash-dotted line) WD models.

nova probably entered the nebular phase about 40 days after the outburst. Strong emission lines such as [O III] may contribute to the visual magnitude and the observational magnitudes gradually deviate from our model light curve.

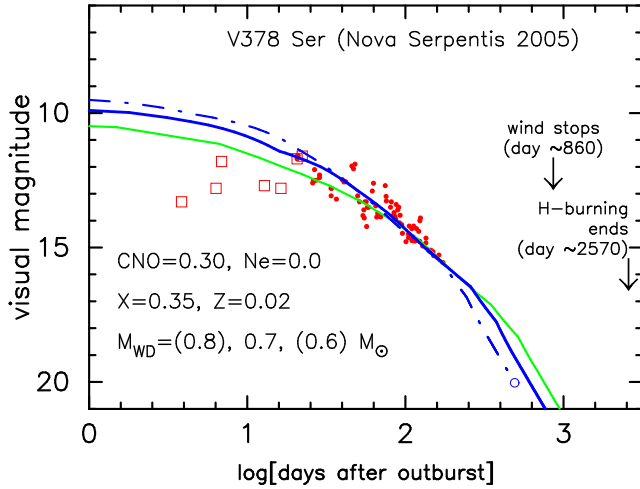


FIG. 8.— The best fit $0.7 M_{\odot}$ WD model (thick solid line) is plotted together with $0.6 M_{\odot}$ (thin solid line) and $0.8 M_{\odot}$ (dash-dotted line) WD models. Here we assume a chemical composition of $X = 0.35$, $X_{\text{CNO}} = 0.30$, and $Z = 0.02$. Dots: visual and V magnitudes taken from AAVSO. Open squares: visual and V observations taken from IAU Circulars 8505, 8506, and 8509.

The estimated WD mass of $1.1 \pm 0.1 M_{\odot}$ exceeds the upper limit for CO white dwarf masses born in a binary, i.e., $M_{\text{CO}} \lesssim 1.07 M_{\odot}$ (e.g., Umeda et al. 1999), so we reexamine light curves with a chemical composition of Ne nova 2, $X = 0.55$, $X_{\text{CNO}} = 0.10$, $X_{\text{Ne}} = 0.03$, and $Z = 0.02$. We have obtained the best-fit model when the WD mass is $1.2 \pm 0.1 M_{\odot}$, as shown in Figure 7.

7. V378 SER (NOVA SERPENTIS 2005)

V378 Serpentis was discovered by Pojmanski in an All Sky Automated Survey (ASAS) image taken on March 18.345 UT (JD 2453447.845) at $V = 13.3$ (Pojmanski et al. 2005a). This nova was not detected (limiting mag 14) on March 14.389 UT (JD 2453443.889) (Pojmanski et al. 2005a), so we assume that JD 2453444.0 (March 14.5 UT) is the outburst day. Adopting an visual magnitude of 11.6 on JD 2453466.2 observed by Yoshida (Schmeer & Yoshida 2005) as the maximum visual magnitude for V378 Ser, we obtain $t_2 = 44$ days and $t_3 = 90$ days.

Our best-fit light curves are plotted in Figure 8 for a chemical composition of CO nova 2, $X = 0.35$, $X_{\text{CNO}} = 0.30$, and $Z = 0.02$. The visual (V) magnitudes are roughly fitted with our model light curve after the optical maximum. The WD mass is estimated to be $0.7 \pm 0.1 M_{\odot}$.

8. V5116 SGR (NOVA SAGITTARII 2005 NO.2)

V5116 Sagittarii was discovered by Liller on July 4.049 UT (JD 2453555.549) at mag about 8.0 (Liller 2005). This object was not detected on June 12 (limiting mag about 11.0), so we assume that JD 2453552.0 (July 1.5 UT) is the outburst day. Adopting an visual magnitude of 8.0 on JD 2453555.5 observed by Liller (Liller 2005) as the maximum visual magnitude for V5116 Sgr, we obtain $t_2 = 20$ days and $t_3 = 33$ days.

Our best-fit light curves are plotted in Figure 9 for a chemical composition of CO nova 2, $X = 0.35$, $X_{\text{CNO}} = 0.30$, and $Z = 0.02$. The visual (V) magnitudes are roughly fitted with our model light curve until about day 30, but are gradually departing from it after that. At this stage, the nova probably entered the transition/nebular phase and the deviation comes from the contribution of strong emission lines. The WD mass is estimated to be $0.9 \pm 0.1 M_{\odot}$.

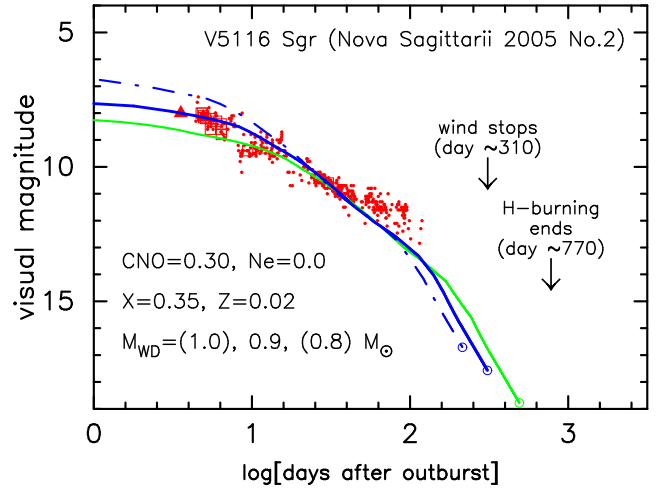


FIG. 9.— The best fit $0.9 M_{\odot}$ WD model (thick solid line) is plotted together with $0.8 M_{\odot}$ (thin solid line) and $1.0 M_{\odot}$ (dash-dotted line) WD models. Here we assume a chemical composition of $X = 0.35$, $X_{\text{CNO}} = 0.30$, and $Z = 0.02$. Dots: visual and V magnitudes taken from AAVSO. Open squares: visual and V observations taken from IAU Circulars 8559, 8561, and 8579. Filled triangles: two discovery magnitudes on a film and on a non-filtered CCD in a digital camera, both taken from IAU Circular 8559.

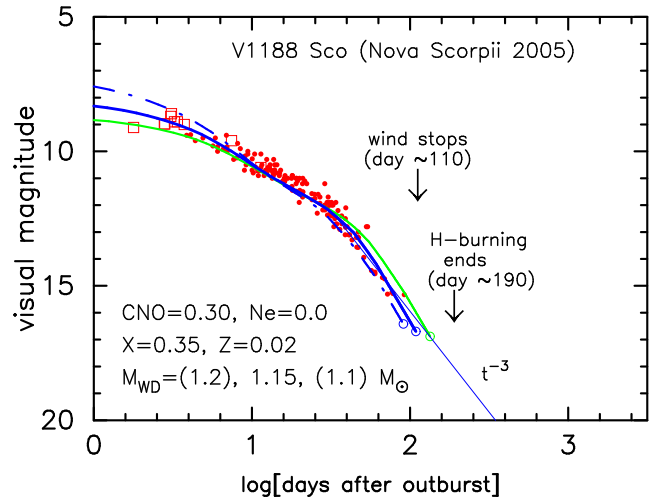


FIG. 10.— The best fit $1.15 M_{\odot}$ WD model (thick solid line) is plotted together with $1.1 M_{\odot}$ (thin solid line) and $1.2 M_{\odot}$ (dash-dotted line) WD models. A straight line of $F_{\lambda} \propto t^{-3}$ is also added after the optically thick wind stops. Here we assume a chemical composition of $X = 0.35$, $X_{\text{CNO}} = 0.30$, and $Z = 0.02$. Dots: visual and V magnitudes taken from AAVSO. Open squares: visual and V observations taken from IAU Circulars 8574, 8575, 8576, and 8581.

9. V1188 SCO (NOVA SCORPII 2005)

V1188 Scorpii was discovered independently by Pojmanski on July 25.284 UT (JD 2453576.784) at $V = 9.11$ and by Nishimura on July 26.565 UT (Pojmanski et al. 2005b). This object was not detected on July 23.287 UT (JD 2453574.787) with limiting mag about 14.0, so we assume that JD 2453575.0 (July 23.5 UT) is the outburst day. Adopting an visual magnitude of 8.6 on JD 2453578.1 observed by Hashimoto & Urata (Pojmanski et al. 2005b) as the maximum visual magnitude for V1188 Sco, we obtain $t_2 = 7$ days and $t_3 = 21$ days.

Our best-fit light curves are plotted for a chemical composition of CO nova 2, $X = 0.35$, $X_{\text{CNO}} = 0.30$, and $Z = 0.02$ in Figure 10, and for a chemical composition of Ne nova 2, $X = 0.55$, $X_{\text{CNO}} = 0.10$, $X_{\text{Ne}} = 0.03$, and $Z = 0.02$ in Figure 11.

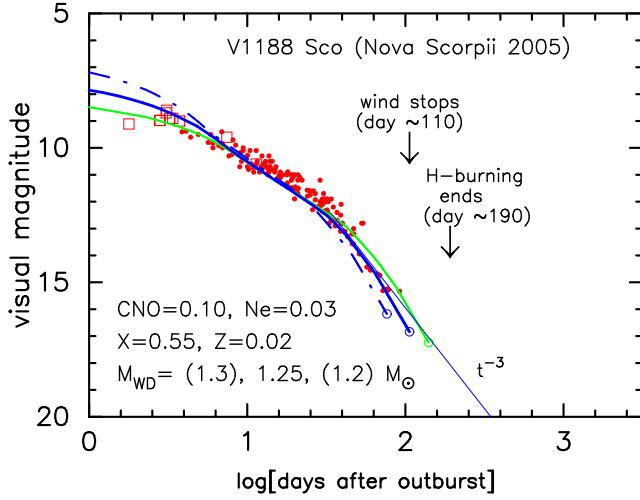


FIG. 11.— Same as in Fig. 10, but for neon novae with a chemical composition of $X = 0.55$, $X_{\text{CNO}} = 0.10$, $X_{\text{Ne}} = 0.03$, and $Z = 0.02$ (model Ne nova 2). The best fit $1.25 M_{\odot}$ WD model (thick solid line) is plotted together with $1.2 M_{\odot}$ (thin solid line) and $1.3 M_{\odot}$ (dash-dotted line) WD models.

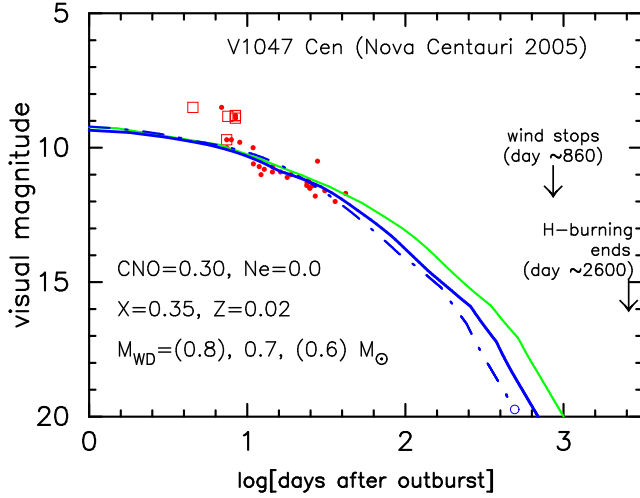


FIG. 12.— The best fit $0.7 M_{\odot}$ WD model (thick solid line) is plotted together with $0.6 M_{\odot}$ (thin solid line) and $0.8 M_{\odot}$ (dash-dotted line) WD models. Here we assume a chemical composition of $X = 0.35$, $X_{\text{CNO}} = 0.30$, and $Z = 0.02$. Dots: visual and V magnitudes taken from AAVSO. Open squares: visual and V observations taken from IAU Circular 8596.

The visual (V) magnitudes are nicely fitted with our model light curves. This indicates that the contribution of emission lines to the V bandpass is not so large. Since the WD mass exceeds the upper limit for CO white dwarf masses born in a binary, i.e., $M_{\text{CO}} \lesssim 1.07 M_{\odot}$ (e.g., Umeda et al. 1999), we may conclude that the WD is an O-Ne-Mg core of $1.25 \pm 0.05 M_{\odot}$.

10. V1047 CEN (NOVA CENTAURI 2005)

V1047 Centauri was discovered by Liller on September 1.031 UT (JD 2453614.531) at mag about 8.5 (Liller et al. 2005a), including no detection of this object on August 12.050 UT (limiting mag about 11). So we assume that JD 2453610.0 (August 27.5 UT) is the outburst day. Adopting an visual magnitude of 8.5 on JD 2453614.531 observed by Liller (Liller et al. 2005a) as the maximum visual magnitude for V1047 Cen, we obtain $t_2 = 6$ days and $t_3 = 26$ days.

Our best-fit light curves are plotted in Figure 12 for a chemical composition of CO nova 2, $X = 0.35$, $X_{\text{CNO}} = 0.30$, and $Z = 0.02$. The visual (V) magnitudes are roughly fitted with

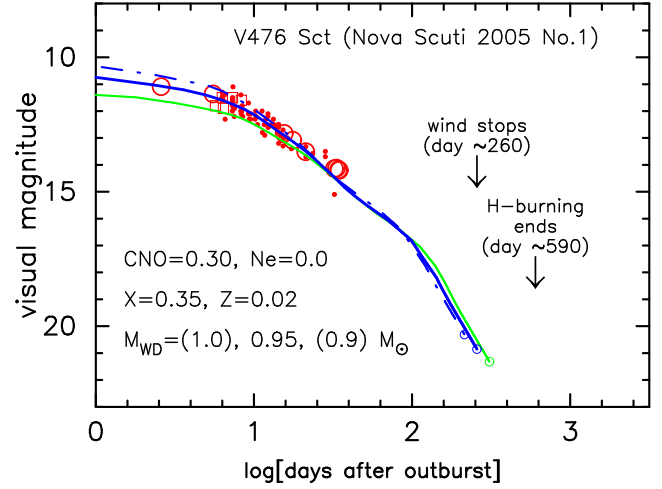


FIG. 13.— The best fit $0.95 M_{\odot}$ WD model (thick solid line) is plotted together with $0.9 M_{\odot}$ (thin solid line) and $1.0 M_{\odot}$ (dash-dotted line) WD models. Here we assume a chemical composition of $X = 0.35$, $X_{\text{CNO}} = 0.30$, and $Z = 0.02$. Dots: visual and V magnitudes taken from AAVSO. Open squares: visual and V observations taken from IAU Circular 8596.

our model light curve except for the early several days. We have already seen, in V1500 Cyg, such a very bright peak more than a magnitude above our modeled light curve (see, e.g., Hachisu & Kato 2006b). The WD mass is estimated to be $0.7 \pm 0.1 M_{\odot}$.

11. V476 SCT (NOVA SCUTI 2005 NO.1)

V476 Scuti was discovered independently by Takao at an apparent magnitude of 10.3 on an unfiltered CCD image taken on September 30.522 UT and by Haseda at magnitude about 10.9 from photographs obtained on September 30.417 UT (Soma et al. 2005). V476 Sct is a fast nova of $t_2 = 15$ and $t_3 = 28$ days and the reddening is estimated to be $E(B-V) = 1.9$ (Munari et al. 2006a).

Munari et al. (2006a) reported that the nova appeared at $V = 11.09$ on ASAS images taken on September 28.09 UT (JD 2453641.59) and declined at $V = 11.36$ on October 1.02 UT (JD 2453644.52), but was not present on September 24.629 UT (JD 2453638.129) with limiting mag of $V > 15.1$. So we assume that JD 2453639.0 (September 25.5 UT) is the outburst day.

Our best-fit light curves are plotted in Figures 13 for a chemical composition of CO nova 2, $X = 0.35$, $X_{\text{CNO}} = 0.30$, and $Z = 0.02$. The visual and V magnitudes are nicely fitted with our model light curve. Here we mainly fit our model light curve with the observation reported in Munari et al. (2006a). This indicates that the contribution of emission lines to the V bandpass is not so large during the early phase until 35 days after the outburst. The WD mass is estimated to be $0.95 \pm 0.05 M_{\odot}$.

12. V1663 AQL (NOVA AQUILAE 2005)

Pojmanski & Oksanen (2005) reported the discovery of V1663 Aquilae in All Sky Automated Survey (ASAS) images taken on June 9.240 UT (JD 2453530.740) shining at $V = 11.05$, including no detection of this nova on June 3.318 UT (JD 2453524.818) with limiting mag of $V > 14$ (Pojmanski & Oksanen 2005). So we assume that JD 2453525.0 is the outburst day. Adopting an visual magnitude of 10.5 on JD 2453531.7 observed by Pojmanski (Pojmanski & Oksanen 2005) as the maximum visual magnitude for V1663 Aql, we obtain $t_2 = 13$ days and $t_3 = 26$ days.

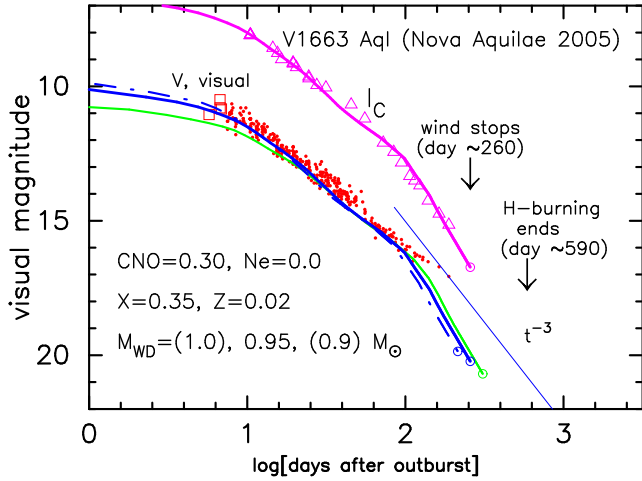


FIG. 14.— The best fit $0.95 M_{\odot}$ WD model (thick solid line) is plotted together with $0.9 M_{\odot}$ (thin solid line) and $1.0 M_{\odot}$ (dash-dotted line) WD models. A straight line of $F_{\lambda} \propto t^{-3}$ is also added after the optically thick wind stops. Here we assume a chemical composition of $X = 0.35$, $X_{\text{CNO}} = 0.30$, and $Z = 0.02$. Dots: visual and V magnitudes taken from AAVSO. Open squares: visual and V observations taken from IAU Circular 8540. Open triangles: I magnitude observations taken from AAVSO.

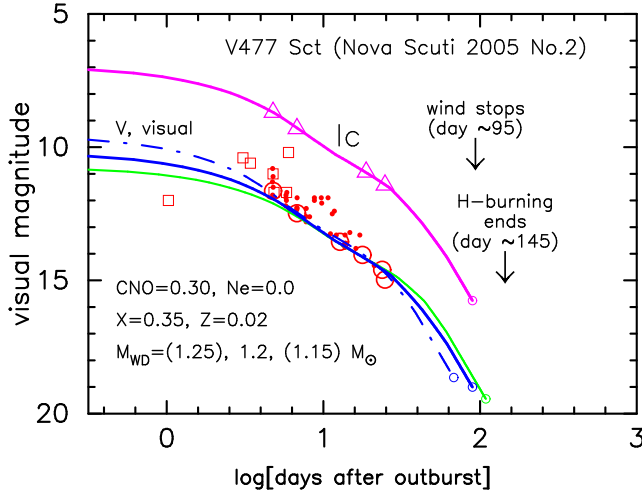


FIG. 15.— The best fit $1.2 M_{\odot}$ WD model (thick solid line) is plotted together with $1.15 M_{\odot}$ (thin solid line) and $1.25 M_{\odot}$ (dash-dotted line) WD models. Here we assume a chemical composition of $X = 0.35$, $X_{\text{CNO}} = 0.30$, and $Z = 0.02$. Dots: visual and V magnitudes taken from AAVSO. Open squares: visual and V observations taken from IAU Circular 8617. Large open circles: V magnitudes taken from Munari et al. (2006b). Open triangles: I_C magnitudes taken from Munari et al. (2006b).

Our best-fit light curves are plotted in Figures 14 for a chemical composition of CO nova 2, $X = 0.35$, $X_{\text{CNO}} = 0.30$, and $Z = 0.02$. The WD mass is estimated to be $0.95 \pm 0.05 M_{\odot}$. Both the visual (V) and I_C magnitudes are nicely fitted with our model light curve. This indicates that the contribution of emission lines to the V bandpass is not so large until about day 100, beyond which the visual magnitudes begins to depart from our model light curve. Puetter et al. (2005) pointed out that the nova has entered the nebular phase 164 days after the outburst.

13. V477 SCT (NOVA SCUTI 2005 NO.2)

V477 Sct was discovered by Pojmanski in All-Sky Automated Survey (ASAS) images on October 11.026 UT (JD 2453654.526) at $V = 12.0$ (Pojmanski et al. 2005c), including no detection of this nova on October 7.055 UT (JD

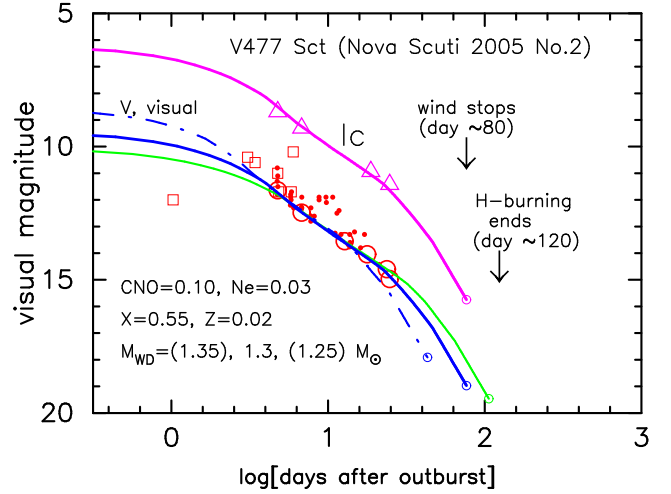


FIG. 16.— Same as in Fig. 15, but for neon novae with a chemical composition of $X = 0.55$, $X_{\text{CNO}} = 0.10$, $X_{\text{Ne}} = 0.03$, and $Z = 0.02$ (model Ne nova 2). The best fit $1.3 M_{\odot}$ WD model (thick solid line) is plotted together with $1.25 M_{\odot}$ (thin solid line) and $1.35 M_{\odot}$ (dash-dotted line) WD models.

2453650.555) with limiting mag $V > 14$. So we assume that JD 2453653.5 (October 10.0 UT) is the outburst day. V477 Sct is a very fast nova of $t_2 = 3$ and $t_3 = 6$ days and the reddening is estimated to be $E(B - V) \geq 1.3$ (Munari et al. 2006b). Munari et al. (2006b) also suggested that the nova was entering a dust condensation episode or brightness oscillations during the transition phase when it became unobservable for the seasonal conjunction with the Sun.

Our best-fit light curves are plotted in Figures 15 for a chemical composition of CO nova 2, $X = 0.35$, $X_{\text{CNO}} = 0.30$, and $Z = 0.02$, and in Figure 16 for a chemical composition of Ne nova 2, $X = 0.55$, $X_{\text{CNO}} = 0.10$, $X_{\text{Ne}} = 0.03$, and $Z = 0.02$. Here we mainly fit our model light curve with the observation by Munari et al. (2006b) both for V and I_C magnitudes. Both the V and I_C magnitudes are nicely fitted with our model light curve except for the early few days. This indicates that the contribution of emission lines to the V bandpass is not so large. The estimated WD mass exceeds the upper limit for CO white dwarf masses born in a binary, i.e., $M_{\text{CO}} \lesssim 1.07 M_{\odot}$ (e.g., Umeda et al. 1999). So we may conclude that the WD is an O-Ne-Mg core of $1.30 \pm 0.05 M_{\odot}$.

Munari et al. (2006b) suggested that this nova resembles Nova LMC 1990 No.1, which at later stages evolved into a neon nova. This is consistent with our result of the massive WD mass ($1.30 \pm 0.05 M_{\odot}$), favorable to an O-Ne-Mg white dwarf. Very high expansion velocities of FWHM = 2900–2600 km s⁻¹ also indicate a high mass WD, being consistent with a $1.30 \pm 0.05 M_{\odot}$ WD.

14. DISCUSSION

We summarize the present fitting results of the light curves in Tables 3 and 4 together with our previous results on three old novae, V1500 Cyg, V1668 Cyg, and V1974 Cyg.

14.1. Dependence on the chemical composition

The light curves based on free-free emission depend not only on the WD mass but also on the chemical composition of a nova envelope. We may have estimated the dependence of the WD mass on the hydrogen content X for the four Ne novae outburst in 2005 by equation (3). For the six CO novae outburst in 2005, we also estimate as

$$M_{\text{WD}}(X) \approx M_{\text{WD}}(0.35) + 0.5(X - 0.35), \quad (5)$$

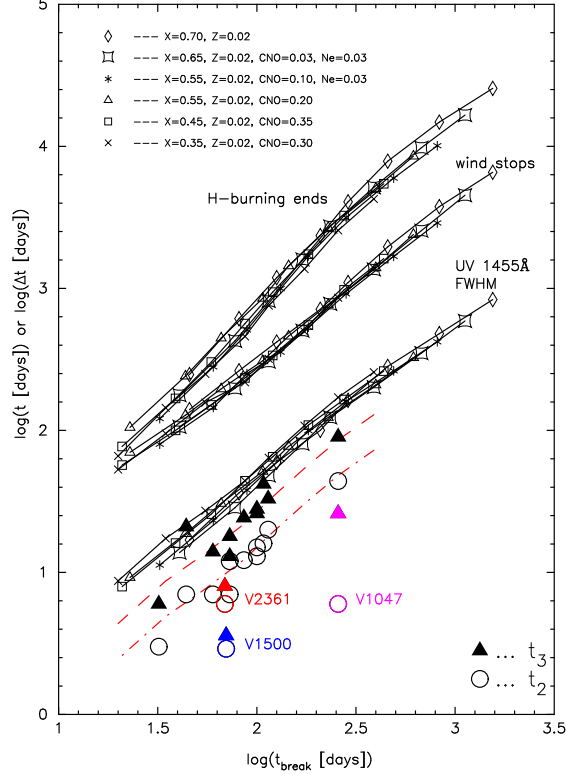


FIG. 17.— Three typical nova timescales of $t_{\text{H-burning}}$, t_{wind} , and $\Delta t_{\text{UV,FWHM}}$ as well as observed t_2 and t_3 are plotted against t_{break} for six different chemical compositions of the nova envelope. Here $t_{\text{H-burning}}$ is the time when hydrogen burning ends, t_{wind} is the time when optically thick winds stop, $\Delta t_{\text{UV,FWHM}}$ is the UV 1455Å duration defined by the full width at the half maximum, and t_{break} is the time of break on the free-free light curve. These timescales depend not only on the WD mass but also on the chemical composition as shown in Hachisu & Kato (2006b). A dashed line denotes an averaged relation given by eq. (6) and a dash-dotted line represents an averaged relation given by eq. (7).

for $0.35 \leq X \leq 0.65$ and $0.06 \leq X_{\text{CNO}} \leq 0.5$. As shown in these equations (3) and (5), the dependence on the hydrogen content is rather small. Therefore, even if the X is unknown, we can roughly estimate the WD mass with an accuracy of about $\pm 0.1 M_{\odot}$.

14.2. Relation among various nova timescales

Cassatella et al. (2002) analyzed the ultraviolet (UV) fluxes of 12 novae well observed with *IUE* and found that the UV outburst duration of their 1455Å continuum band is linearly increasing with the t_3 time for these novae (one exception of V705 Cas because of dust formation). Since our model of the UV 1455Å flux follows well the observed UV fluxes as already shown in Figures 15 (V1668 Cyg) and 21 (V1973 Cyg) of Paper I, we plot t_2 and t_3 against t_{break} in Figure 17 for new novae in 2005 as well as our already studied novae. Many of the points (filled triangles) are aligned on a dashed line, which is described by

$$t_3 = (0.6 \pm 0.08) \langle \Delta t_{\text{UV,FWHM}} \rangle. \quad (6)$$

This means that Cassatella et al.'s result derived from the *IUE* novae also stands for the novae newly outburst in 2005, although equation (6) is somewhat different from Cassatella et al.'s equation (4). Here, $\langle \Delta t_{\text{UV,FWHM}} \rangle$ is an averaged value of our models for various chemical compositions. We can also

obtain the relation between t_2 and t_3 as

$$t_2 = (0.6 \pm 0.08) t_3. \quad (7)$$

Here we have excluded three novae, V1500 Cyg, V2361 Cyg, and V1047 Cen, from this analysis because V1500 Cyg and V1047 Cen are super bright novae discussed below and the light curve of V2361 Cyg is clearly affected by a dust black-out. This relation is essentially the same as the empirical relation given by Capaccioli et al. (1990), i.e.,

$$t_3 = (1.68 \pm 0.08) t_2 + (1.9 \pm 1.5) \text{ days, for } t_3 < 80 \text{ days,} \quad (8)$$

and

$$t_3 = (1.68 \pm 0.04) t_2 + (2.3 \pm 1.6) \text{ days, for } t_3 > 80 \text{ days,} \quad (9)$$

which were already explained in terms of our universal decline law (see Paper I).

14.3. Expansion velocity of nova shell

We plot expansion velocities of each nova in Figure 18. Classical novae usually have many velocity systems such as principal, Orion, diffuse-enhanced, and so on (see, e.g., Payne-Gaposchkin 1957). However, what we are interested in is the expansion velocity for a majority of nova ejecta. So, we adopt the expansion velocity of each nova shell if it is available. Such a nova shell has been detected in three of the four old novae as listed in Table 5.

Velocities of our optically thick winds vary with time (e.g., Kato & Hachisu 1994). Figure 18 shows a maximum expansion velocity of our wind solution for each WD mass. The velocity increases with the WD mass. These three novae, GK Per, V1500 Cyg, and V1974 Cyg, are in good agreement with the velocity of our model. Since no nova shell is observed in V1668 Cyg, we adopt an averaged expansion velocity given by Stickland et al. (1981), which is a bit smaller than our value. This shows that majority of ejecta in nova shells are expanding with the wind velocity of our model.

It should be noted that our wind model are calculated by assuming spherical symmetry. On the other hand, nova shells are not spherical but usually show patchy structures, indicating that high velocity components of novae are coming from gas which goes through low density regions between patchy structures (Kato & Hachisu 2004).

The FWHM of H α lines are plotted for new novae outburst in 2005. These velocities may not be the expansion velocity of nova shell but show a trend of expansion velocities. We can see that the expansion velocity of our model follows the lower bound of these H α line widths. This supports our hypothesis that a majority of ejecta are expanding with our theoretical wind velocities.

14.4. Peak luminosities

Closely looking at the light curve fittings, we have seen two types of light curves at/near the optical maximum: one is the case that our universal decline law reasonably follows the optical peak. Nine of ten novae in 2005 correspond to this type. V1047 Cen is an exception. Three of four old novae, V1668 Cyg, V1974 Cyg, and GK Per, are in this category, but V1500 Cyg is another exception. These two exceptions show that the peak brightness is much brighter than our universal decline law. V1500 Cyg is one of the fastest novae and has been categorized into a group of super bright novae (della Valle 1991). The peak is $m_{V,\text{max}} = 1.85$ and about 2

TABLE 4
LIGHT CURVE PARAMETERS OF NOVAE IN 2005

object	WD mass (M_{\odot})	t_2 (days)	t_3 (days)	t_{break} (days)	t_{wind} (days)	$t_{\text{H-burning}}$ (days)
V2361 Cyg	1.05 ± 0.15	6 ^b	8 ^b	69	169	340
V382 Nor	1.15 ± 0.15	12	18	73	182	382
V5115 Sgr	1.20 ± 0.1	7	14	60	145	280
V378 Ser	0.70 ± 0.1	44	90	257	858	2560
V5116 Sgr	0.90 ± 0.1	20	33	114	319	757
V1188 Sco	1.25 ± 0.05	7	21	44	110	190
V1047 Cen	0.70 ± 0.1	6	26	257	858	2560
V476 Sct	0.95 ± 0.05	15 ^c	28 ^c	100	260	590
V1663 Aql	0.95 ± 0.05	13	26	100	260	590
V477 Sct	1.30 ± 0.05	3 ^d	6 ^d	32	80	121

^a taken from Downes & Duerbeck (2000)

^b already affected by dust formation

^c taken from Munari et al. (2006b)

^d taken from Munari et al. (2006a)

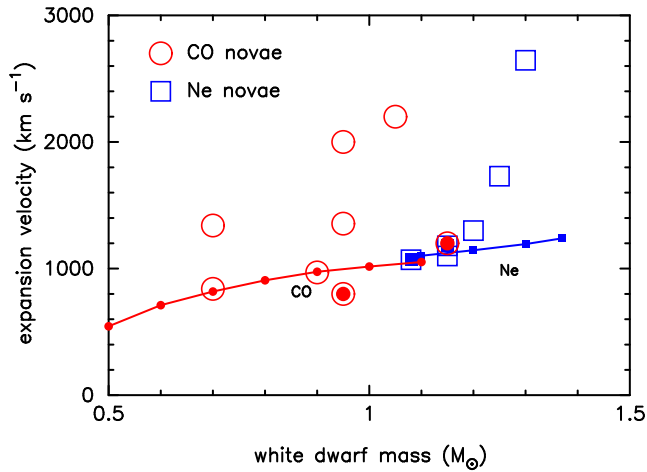


FIG. 18.— Expansion velocity of each nova is plotted against the white dwarf mass. *Large open circles*: the FWHM velocity of $H\alpha$ for each CO nova in Table 6. *Large open squares*: the FWHM velocity of $H\alpha$ for each Ne nova in Table 6. *Large open circles with a filled circle*: the observed expansion velocity of the CO nova shell tabulated in Table 5. *Large open squares with a filled square*: the observed expansion velocity of the Ne nova shell tabulated in Table 5. *Solid line with small filled circles*: the wind velocity of our spherically symmetric nova model with a chemical composition of CO nova 2. *Solid line with small filled squares*: the wind velocity of our spherically symmetric nova model with a chemical composition of Ne nova 2. The wind velocities of these spherically symmetric models seem to follow the lower boundary of the observed expansion velocities.

mag brighter than our universal decline law as shown in Figure 13 of Hachisu & Kato (2006b). The peak of V1047 Cen is also about 1.5 mag brighter than our universal decline law as in Figure 12. Its light curve is similar to that of GQ Mus 1983, rather than V1500 Cyg. We do not understand the physical reason of such a large deviation of these novae from our universal law. It is one of the targets of our future research.

15. CONCLUSIONS

Our main results are summarized as follows:

1. The template light curves (Hachisu & Kato 2006b, Paper I) are applied to GK Per 1901 and recent 10 novae that outbursted in 2005. We have confirmed that the universal decline law described in Paper I is also well applicable to these novae. The estimated WD masses are $1.15 M_{\odot}$ (GK Per), $1.05 M_{\odot}$ (V2361 Cyg), $1.15 M_{\odot}$ (V382 Nor), $1.2 M_{\odot}$ (V5115 Sgr), $0.7 M_{\odot}$ (V378 Ser), $0.9 M_{\odot}$ (V5116 Sgr), $1.25 M_{\odot}$ (V1188 Sco), $0.7 M_{\odot}$ (V1047 Cen), $0.95 M_{\odot}$ (V476 Sct), $0.95 M_{\odot}$

TABLE 5
SHELL EXPANSION VELOCITIES OF FOUR NOVAE ALREADY STUDIED

object	expansion velocity (km s^{-1})	reference
GK Per 1901	1200	Cohen & Rosenthal (1983)
V1500 Cyg 1975	1180	Cohen (1985)
V1668 Cyg 1978	760 ^a	Stickland et al. (1981)
V1974 Cyg 1992	1070	Downes & Duerbeck (2000)

^a an average expansion velocity of nebula because no shell has been detected yet

(V1663 Aql), and $1.30 M_{\odot}$ (V477 Sct), within a rough accuracy of $\pm 0.1 M_{\odot}$.

2. Four (V382 Nor, V5115 Sgr, V1188 Sco, and V477 Sct) of ten novae in the year 2005 are probably neon novae on an O-Ne-Mg WD mainly because their WD masses exceed $1.07 M_{\odot}$, which is an upper limit mass of CO cores born in binaries (Umeda et al. 1999).

3. Estimated WD masses depend weakly on the chemical composition (especially on the hydrogen content X), i.e., the above WD masses increase by $+0.5(X-0.35) M_{\odot}$ for the six CO novae and by $+0.5(X-0.55) M_{\odot}$ for the four neon novae. These WD masses should be corrected when their chemical compositions will be determined in future.

4. Two (V1500 Cyg and V1047 Cen) of our 14 studied novae show a 1.5–2 mag brighter peak than our universal decline law. These two are categorized into the super bright novae (della Valle 1991). On the other hand, the residual 12 novae are in the normal bright novae. The physical reason for super bright novae is not understood yet.

5. We have confirmed linear relations between $\Delta t_{\text{UV,FWHM}}$ and t_3 , i.e., $t_3 = (0.6 \pm 0.08) \langle \Delta t_{\text{UV,FWHM}} \rangle$, which was first pointed out by Cassatella et al. (2002), and between t_2 and t_3 , i.e., $t_2 = (0.6 \pm 0.08) t_3$, which was already proposed by Capaccioli et al. (1990).

6. The observed expansion velocities of nova shells are well reproduced with our wind model for three old novae, GK Per, V1500 Cyg, and V1974 Cyg.

We thank the American Association of Variable Star Observers (AAVSO) for the visual data of recent novae outbursted in 2005. This research has been supported in part by the Grant-in-Aid for Scientific Research (16540211, 16540219) of the Japan Society for the Promotion of Science.

REFERENCES

- Ayani, K., & Kawabata, Y. 2005, IAU Circ., 8501, 3
 Campbell, L. 1903, Annals of Harvard College Observatory, 48, 39
 Capaccioli, M., della Valle, M., D’Onofrio, M., Rosino, L. 1990, ApJ, 360, 63
 Cassatella, A., Altamore, A., & González-Riestra, R. 2002, A&A, 384, 1023
 Child, L. 1901, MNRAS, 61, 483
 Cohen, J. G. 1985, ApJ, 292, 90
 Cohen, J. G., & Rosenthal, A. J. 1983, ApJ, 268, 689
 della Valle, M. 1991, A&A, 252, L9
 Downes, R. A., & Duerbeck, H. W. 2000, AJ, 120, 2007
 Ennis, D., Becklin, E. E., Beckwith, S., Elias, J., Gatley, I., Matthews, K., Neugebauer, G., & Willner, S. P. 1977, ApJ, 214, 478
 Ederoclite, A., Mason, E., & Dall, T. H. 2005a, IAU Circ., 8497, 2
 Fujii, M., & Yamaoka, H. 2005, IAU Circ., 8617, 3

TABLE 6
EXPANSION VELOCITIES OF NOVAE IN 2005

object	WD mass (M_{\odot})	days after outburst	$H\alpha^a$ (km s^{-1})	O I 8446 \AA^a (km s^{-1})	reference
V2361 Cyg	1.05 ± 0.15	5	3200	...	Naito et al. (2005a)
		28	...	2600	Russell et al. (2005b)
		82–85	2200	2000	Gaggero et al. (2005)
V382 Nor	1.15 ± 0.15	~ 10	1100	...	Ederoclite et al. (2005a)
V5115 Sgr	1.20 ± 0.1	2	1300	...	Ayani & Kawabata (2005)
V378 Ser	0.70 ± 0.1	21	1100	...	Yamaoka & Fujii (2005)
V5116 Sgr	0.90 ± 0.1	5	970	...	Liller (2005)
		15	...	2200	Russell et al. (2006a)
V1188 Sco	1.25 ± 0.05	4	1730	...	Naito et al. (2005b)
V1047 Cen	0.70 ± 0.1	8	840	...	Liller et al. (2005a)
V476 Sct	0.95 ± 0.05	32	1355	1170	Munari et al. (2006a)
V1663 Aql	0.95 ± 0.05	164	2000	...	Puetter et al. (2005)
V477 Sct	1.30 ± 0.05	6	2900	...	Fujii & Yamaoka (2005)
		18	2645	2590	Munari et al. (2006b)
		36	2700	...	Mazuk et al. (2005)

^a The full width at half maximum (FWHM) is adopted as the expansion velocity

- Gaggero, D., Martire, I., Poggiani, R., Puccetti, V., Shore, S. N., Tognelli, E., Bernabei, S. 2005, IAU Circ., 8529, 1
- Gallagher, J. S., & Ney, E. P. 1976, ApJ, 204, L35
- Gore, J. E. 1901, MNRAS, 62, 156
- Grevesse, N., & Anders, E. 1989, Cosmic Abundances of Matter, ed. C. J. Waddington (New York: AIP), 1
- Hachisu, I., & Kato, M. 2001b, ApJ, 558, 323
- Hachisu, I., & Kato, M. 2005, ApJ, 631, 1094
- Hachisu, I., & Kato, M. 2006a, ApJ, 642, L53
- Hachisu, I., & Kato, M. 2006b, ApJS, 167, 59 (Paper I)
- Hachisu, I., et al. 2006, ApJ, 651, L141
- Kato, M. 1997, ApJS, 113, 121
- Kato, M. 1999, PASJ, 51, 525
- Kato, M., & Hachisu, I., 1994, ApJ, 437, 802
- Kato, M., & Hachisu, I., 2004, ApJ, 587, L39
- Kawara, K., Maihara, T., Noguchi, K., Oda, N., Sato, S., Oishi, M., & Iijima, T. 1976, PASJ, 28, no. 1, 1976, p. 163
- Krautter, J., Ögelman, H., Starrfield, S., Wichmann, R., & Pfeffermann, E. 1996, ApJ, 456, 788
- Liller, W. 2005, IAU Circ., 8559, 1
- Liller, W., Jacques, C., Pimentel, E., Aguiar, J. G. de S., Shida, R. Y. 2005a, IAU Circ., 8596, 1
- Liller, W., Monard, L. A. G., Africa, S., Samus, N. N., Kazarovets, E. 2005b, IAU Circ., 8497, 1
- Livio, Mario; Truran, James W. 1994, ApJ, 425, 797
- Mallama, A. D., & Skillman, D. R. 1979, PASP, 91, 99
- Mazuk, S., Lynch, D. K., Rudy, R. J., Venturini, C. C., Puetter, R. C., Perry, R. B., & Walp, B. 2005, IAU Circ., 8644, 1
- McLaughlin, D. B. 1949, Publ. of the Obs. of the Univ. of Michigan, 9, 13
- McLaughlin, D. B. 1960, in Stellar Atmospheres, ed. J. L. Greenstein (The University of Chicago Press: Chicago), 585.
- Morales-Rueda, L., Still, M. D., Roche, P., Wood, J. H., Lockley, J. J. 2002, MNRAS, 329, 597
- Munari, U., Henden, A., Pojmanski, G., Dallaporta, S., Siviero, A., & Navasardyan, H. 2006a, MNRAS, 369, 1755
- Munari, U., Siviero, A., Navasardyan, H., & Dallaporta, S. 2006b, A&A, 452, 567
- Naito, H., Tokimasa, N., & Yamaoka, H. 2005a, IAU Circ., 8484, 1
- Naito, H., Tokimasa, N., & Yamaoka, H. 2005b, IAU Circ., 8576, 2
- Nakano, S., Kadota, K., & Wakuda, S. 2005a, IAU Circ., 8501, 1
- Nakano, S., Nishimura, H., Sakurai, Y., & Yamaoka, H. 2005b, IAU Circ., 8500
- Nakano, S.; Nishimura, H.; Wakuda, S.; Kadota, K. 2005c, IAU Circ., 8483, 1
- Payne-Gaposchkin, C. 1957, The Galactic Novae (Amsterdam: North-Holland)
- Pojmanski, G., Masi, G., & Wilcox, R. 2005a, IAU Circ., 8505, 1
- Pojmanski, G., Nakano, S., Nishimura, H., Hashimoto, N., & Urata, T. 2005b, IAU Circ., 8574, 1
- Pojmanski, G., & Oksanen, A. 2005, IAU Circ., 8540, 1
- Pojmanski, G., Yamaoka, H., Haseda, K., Puckett, T., Hornoch, K., Schmeer, P., & Samus, N. N. 2005c, IAU Circ., 8617, 1
- Pottasch, S. 1959, Annales d'Astrophysique, 22, 412
- Puetter, R. C., Rudy, R. J., Lynch, D. K., Mazuk, S., Venturini, C. C., Perry, R. B., & Walp, B. 2005, IAU Circ., 8640, 2
- Rambaut, A. A. 1901a, MNRAS, 61, 348
- Rambaut, A. A. 1901b, MNRAS, 61, 390
- Rambaut, A. A. 1901c, MNRAS, 61, 467
- Rambaut, A. A. 1901d, MNRAS, 61, 544
- Rambaut, A. A. 1901e, MNRAS, 62, 78
- Rambaut, A. A. 1902, MNRAS, 62, 586
- Rambaut, A. A. 1903, MNRAS, 63, 509
- Reinsch, K. 1994, A&A, 281, 108
- Russell, R. W., Rudy, R. J., Lynch, D. K., Golisch, W. 2005b, IAU Circ., 8524, 2
- Russell, R. W., Rudy, R. J., & Lynch, D. K. 2006a, IAU Circ., 8579, 4
- Sabbadin, F., & Bianchini, A. 1983, A&AS, 54, 393
- Schmeer, P., & Yoshida, S. 2005, IAU Circ., 8509, 4
- Sharp, M. C. 1901, MNRAS, 61, 398
- Slavin, A. J., O'Brien, T. J., Dunlop, J. S. 1995, MNRAS, 276, 353
- Soma, M., Takao, A., Yamaoka, H., Haseda, K., Gilmore, A. C., Kilmartin, P. M., Nakano, S., & Kadota, K. 2005, IAU Circ., 8607, 1
- Stickland, D. J., Penn, C. J., Seaton, M. J., Snijders, M. A. J., & Storey, P. J. 1981, MNRAS, 197, 107
- Umeda, H., Nomoto, K., Yamaoka, H., & Wanajo, S. 1999, ApJ, 513, 861
- Venturini, C. C., Rudy, R. J., Lynch, D. K., Mazuk, S., Puetter, R. C., Perry, R. B., & Walp, B. 2005, IAU Circ., 8641, 2
- Warner, B. 1986, MNRAS, 222, 11
- Warner, B. 1995, Cataclysmic variable stars, Cambridge,
- Williams, A. S. 1901a, MNRAS, 61, 337
- Williams, A. S. 1901b, MNRAS, 61, 396
- Williams, A. S. 1901b, MNRAS, 61, 480
- Williams, A. S. 1901d, MNRAS, 61, 550
- Williams, A. S. 1902, MNRAS, 62, 589
- Williams, A. S. 1919, MNRAS, 79, 362
- Williams, R. E., Hamuy, M., Phillips, M. M., Heathcote, S. R., Wells, L., & Navarrete, M. 1991, ApJ, 376, 721
- Williams, R. E. 1994, ApJ, 426, 279
- Woodward, C. E., Gehrz, R. D., Jones, T. J., Lawrence, G. F., & Skrutskie, M. F. 1997, ApJ, 477, 817
- Wu, C.-C., Holm, A. V., Panek, R. J., Raymond, J. C., Hartmann, L. W., & Swank, J. H. 1989, ApJ, 339, 443
- Yamaoka, H., & Fujii, M. 2005, IAU Circ., 8506, 3